



## A DENSITY FUNCTIONAL THEORY STUDY OF GEOMETRICAL AND ELECTRONIC PROPERTIES OF FERROCENE AND ACETYL FERROCENE

Sabyasachi Khatua

Department of Chemistry, YS Palpara Mahavidyalaya, Palpara, Purba Medinipur, West Bengal, India

\*Corresponding author: [skhatua1@gmail.com](mailto:skhatua1@gmail.com)

### ABSTRACT

Studies on substituted ferrocenes, acetyl ferrocene in particular, are very limited. So the geometrical and electrical properties of ferrocene and acetyl ferrocene are studied using Density Functional Theory (DFT) with particular emphasis on Natural Bond Orbital (NBO) and Time Dependent Density Functional Theory (TDDFT) analysis. In the gas phase the eclipsed conformer is found to be more stable than the corresponding staggered conformer for both the title compounds. Mulliken charge analysis is carried out to identify the distribution of atomic charge on various atoms of both the molecules. From the Frontier Molecular Orbital (FMO) analysis, the HOMO-LUMO energy gaps of the eclipsed conformers of ferrocene and acetyl ferrocene are calculated as 5.42 and 4.62 eV respectively. Molecular electrostatic potential (MEP) is used to identify the potential active sites which are susceptible to nucleophilic and electrophilic attacks. Natural population analysis is carried out to find the distribution of electrons in the core, valence and Rydberg sub-shells of both compounds. Thus NBO analysis provides useful information regarding intra- and intermolecular bonding and interactions among various bonds within the molecule. Finally TDDFT calculations are performed and UV-VIS spectra are simulated. This helps us to identify the important electronic transitions between various energy levels. This study provides a better understanding of the charge delocalization process and electronic properties of ferrocene and acetyl ferrocene to a greater extent.

**Keywords:** Density Functional Theory (DFT), Natural Bond Orbital (NBO), Time Dependent Density Functional Theory (TDDFT), Molecular Electrostatic Potential (MEP), UV-VIS spectra, Mulliken charge, Charge transfer.

### 1. INTRODUCTION

The study of ferrocene and substituted ferrocene compounds has drawn much attention over the last few decades because of their wide applications in various fields of science and technology such as homogeneous catalysis, molecular sensing, polymer chemistry and optical materials [1]. Ferrocene normally exists in two conformers, namely, eclipsed ( $D_{5h}$  symmetry) and staggered ( $D_{5d}$  symmetry). Previous studies reveal that staggered structure is mainly observed in the condensed phase [2-5] whereas the eclipsed structure is found in the gas phase [6-8]. It is observed that eclipsed conformer is the global minimum structure whereas the staggered conformer is the saddle point in gas phase [9]. Remarkably in presence of a few electron donating substituents, the staggered structure appears to be somewhat stabilized as compared to the corresponding eclipsed structure [10]. The d electrons of iron play an important role in characterizing the properties of ferrocene [11].

Although ferrocene have been studied widely and studies of a few substituted ferrocenes are also available, no detailed theoretical study on acetyl ferrocene is available to date. In the present paper we focus to study the structure of ferrocene and how replacement of a hydrogen atom by an acetyl group changes the geometrical and electronic properties of ferrocene. Particular emphasis is given on the Natural Bond Orbital (NBO) analysis of both ferrocene and acetyl ferrocene with a view to explain their electronic properties.

### 2. COMPUTATIONAL METHODS

All calculations are performed in the gas phase using Gaussian 09 software package [12] within the framework of Density Functional Theory (DFT). Gauss View [13] is used as the molecular visualization program. Geometry optimizations of the eclipsed and staggered conformers of both ferrocene and acetyl ferrocene are performed using Becke, 3-parameter Lee, Yang and Parr (B3LYP) model with 6-31G\* basis set. A previous study [10]

shows that 6-31G\* basis set produces satisfactory results in case of ferrocene and substituted ferrocenes. Various interactions between the atoms of the title compounds are studied by Natural Bond Orbital (NBO) method. All NBO calculations are performed with NBO 3.1 programme as executed by Gaussian 09W software. The UV-VIS spectra of the B3LYP/6-31G\* optimized geometries are simulated using Gaussian 09W package within the framework of Time Dependent Density Functional Theory (TDDFT).

### 3. RESULTS AND DISCUSSION

#### 3.1. Analysis of geometrical parameters

The optimized energies of the eclipsed and staggered conformers of ferrocene are calculated to be -1650.68972541 a.u. and -1650.68950336 a.u. respectively. The difference in energy between the two conformers is approximately 0.58 kJ/mol. This result is in conformity with the experimental result [14] which suggests that in the gas phase eclipsed conformer is more stable than the staggered conformer. The optimized energies of the eclipsed and staggered conformers of acetyl ferrocene are calculated as -1803.33648354 and -1803.33617119 a.u. respectively. This clearly indicates that even for acetyl ferrocene, in the gas phase the eclipsed conformer is more stable than the staggered conformer. The difference in energy between the two conformers is approximately 0.82 kJ/mol. Therefore substitution of a hydrogen atom of ferrocene by an acetyl group provides additional stability to the eclipsed conformer.

The bond lengths of the optimized eclipsed and staggered conformers of ferrocene and acetyl ferrocene are shown in table 1. It shows that the optimized bond lengths of the eclipsed conformer of ferrocene are nearly the same as that of the corresponding staggered

conformer. When the hydrogen atom of C<sub>11</sub> is replaced by an acetyl group, the effect of substitution is more significant on the substituted cyclopentadienyl ring (SCp) than on the unsubstituted ring (Cp). On the SCp ring, the effect is particularly confined to the bonds adjoining C<sub>11</sub> atom-both in case of eclipsed and staggered conformers of acetyl ferrocene. In case of eclipsed acetyl ferrocene, the (C<sub>7</sub> - C<sub>11</sub>) and (C<sub>10</sub> - C<sub>11</sub>) bond lengths have increased slightly to 1.4370 and 1.4398 Å respectively. The Fe-C (ring) bond distances of ferrocene are almost uniform. In case of acetyl ferrocene, distances of Fe-C (Cp ring) bonds are almost uniform whereas those of Fe-C (SCp ring) bonds are rather inconsistent. This indicates that the effect of substitution is predominant on the Fe-C bonds of the SCp ring only. This trend is exactly the same for both conformers of acetyl ferrocene.

#### 3.2. Mulliken charge analysis

The electronic structure of a molecule is greatly influenced by the distribution of atomic charge on various atoms of the molecule [15, 16]. This distribution of charge is very important in the sense that it helps to identify the donor and acceptor centres within the molecule which are involved in any kind of charge transfer processes. The distribution of electronic charge of the eclipsed conformers of ferrocene and acetyl ferrocene are listed in table 2.

Mulliken charge analysis shows that, for both ferrocene and acetyl ferrocene, all the ring carbon atoms bear a negative charge whereas the iron atom has a positive charge. In ferrocene, the distribution of charge is almost uniform on both the rings. But in case of acetyl ferrocene, distribution of charge is rather non-uniform, particularly on the carbon atoms of the SCp ring.

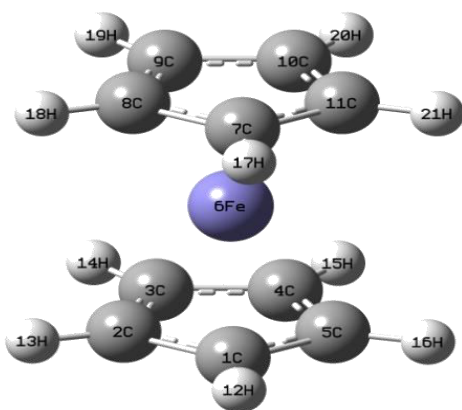


Fig. 1: Eclipsed ferrocene

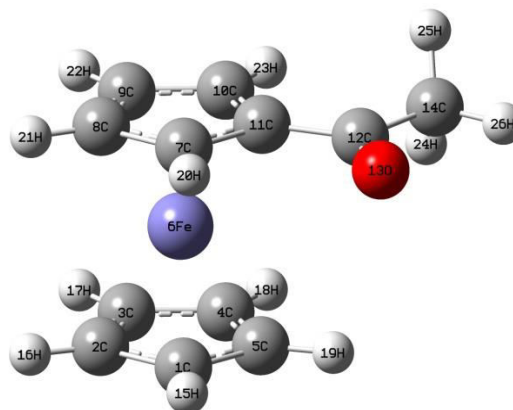


Fig. 2: Eclipsed acetyl ferrocene

**Table 1: Bond lengths of the optimized geometries of the eclipsed and staggered conformers of ferrocene and acetyl ferrocene in Å**

Bonds	Ferrocene		Bonds	Acetyl ferrocene	
	Eclipsed (Å)	Staggered (Å)		Eclipsed (Å)	Staggered (Å)
R(C <sub>1</sub> - C <sub>2</sub> )	1.4284	1.4281	R(1,2)	1.4284	1.4264
R(C <sub>2</sub> - C <sub>3</sub> )	1.4285	1.4280	R(2,3)	1.4281	1.4292
R(C <sub>3</sub> - C <sub>4</sub> )	1.4283	1.4281	R(C <sub>3</sub> - C <sub>4</sub> )	1.4285	1.4271
R(C <sub>4</sub> - C <sub>5</sub> )	1.4285	1.4280	R(C <sub>4</sub> - C <sub>5</sub> )	1.4282	1.4275
R(C <sub>5</sub> - C <sub>1</sub> )	1.4286	1.4281	R(C <sub>5</sub> - C <sub>1</sub> )	1.4272	1.4280
R(C <sub>7</sub> - C <sub>8</sub> )	1.4284	1.4280	R(C <sub>7</sub> - C <sub>8</sub> )	1.4215	1.4234
R(C <sub>8</sub> - C <sub>9</sub> )	1.4284	1.4280	R(C <sub>8</sub> - C <sub>9</sub> )	1.4300	1.4296
R(C <sub>9</sub> - C <sub>10</sub> )	1.4284	1.4280	R(C <sub>9</sub> - C <sub>10</sub> )	1.4238	1.4211
R(C <sub>10</sub> - C <sub>11</sub> )	1.4286	1.4280	R(C <sub>10</sub> - C <sub>11</sub> )	1.4398	1.4366
R(C <sub>11</sub> - C <sub>7</sub> )	1.4285	1.4280	R(C <sub>11</sub> - C <sub>7</sub> )	1.4370	1.4395
R(Fe - C <sub>1</sub> )	2.0535	2.0553	R(Fe - C <sub>1</sub> )	2.0561	2.0571
R(Fe - C <sub>2</sub> )	2.0533	2.0539	R(Fe - C <sub>2</sub> )	2.0528	2.0543
R(Fe - C <sub>3</sub> )	2.0539	2.0542	R(Fe - C <sub>3</sub> )	2.0537	2.0556
R(Fe - C <sub>4</sub> )	2.0544	2.0551	R(Fe - C <sub>4</sub> )	2.0578	2.0598
R(Fe - C <sub>5</sub> )	2.0540	2.0553	R(Fe - C <sub>5</sub> )	2.0586	2.0586
R(Fe - C <sub>7</sub> )	2.0537	2.0540	R(Fe - C <sub>7</sub> )	2.0469	2.0495
R(Fe - C <sub>8</sub> )	2.0536	2.0556	R(Fe - C <sub>8</sub> )	2.0633	2.0618
R(Fe - C <sub>9</sub> )	2.0538	2.0552	R(Fe - C <sub>9</sub> )	2.0603	2.0638
R(Fe - C <sub>10</sub> )	2.0540	2.0546	R(Fe - C <sub>10</sub> )	2.0474	2.0468
R(Fe - C <sub>11</sub> )	2.0537	2.0539	R(Fe - C <sub>11</sub> )	2.0461	2.0475
			R(C <sub>11</sub> - C <sub>12</sub> )	1.4813	1.4815
			R(C <sub>12</sub> - O <sub>13</sub> )	1.2230	1.2230
			R(C <sub>12</sub> - C <sub>14</sub> )	1.5209	1.5209
R(C <sub>1</sub> - H <sub>12</sub> )	1.0823	1.0823	R(C <sub>1</sub> - H <sub>15</sub> )	1.0819	1.0823
R(C <sub>2</sub> - H <sub>13</sub> )	1.0822	1.0823	R(C <sub>2</sub> - H <sub>16</sub> )	1.0822	1.0821
R(C <sub>3</sub> - H <sub>14</sub> )	1.0822	1.0823	R(C <sub>3</sub> - H <sub>17</sub> )	1.0822	1.0823
R(C <sub>4</sub> - H <sub>15</sub> )	1.0822	1.0823	R(C <sub>4</sub> - H <sub>18</sub> )	1.0822	1.0823
R(C <sub>5</sub> - H <sub>16</sub> )	1.0822	1.0823	R(C <sub>5</sub> - H <sub>19</sub> )	1.0824	1.0822
R(C <sub>7</sub> - H <sub>17</sub> )	1.0823	1.0823	R(C <sub>7</sub> - H <sub>20</sub> )	1.0808	1.0819
R(C <sub>8</sub> - H <sub>18</sub> )	1.0822	1.0824	R(C <sub>8</sub> - H <sub>21</sub> )	1.0823	1.0824
R(C <sub>9</sub> - H <sub>19</sub> )	1.0822	1.0823	R(C <sub>9</sub> - H <sub>22</sub> )	1.0823	1.0823
R(C <sub>10</sub> - H <sub>20</sub> )	1.0822	1.0823	R(C <sub>10</sub> - H <sub>23</sub> )	1.0819	1.0808
R(C <sub>11</sub> - H <sub>21</sub> )	1.0822	1.0823	R(C <sub>14</sub> - H <sub>24</sub> )	1.0966	1.0965
			R(C <sub>14</sub> - H <sub>25</sub> )	1.0972	1.0972
			R(C <sub>14</sub> - H <sub>26</sub> )	1.0917	1.0917

**Table 2: Mulliken atomic charges on the atoms of ferrocene and acetyl ferrocene**

Eclipsed Ferrocene			Eclipsed Acetyl ferrocene		
Atom label	Symbol	Charge	Atom label	Symbol	Charge
1	C	-0.193802	1	C	-0.190126
2	C	-0.193837	2	C	-0.193391
3	C	-0.193903	3	C	-0.192339
4	C	-0.193811	4	C	-0.195865
5	C	-0.193940	5	C	-0.193203
6	Fe	0.468218	6	Fe	0.468569
7	C	-0.193743	7	C	-0.208188
8	C	-0.193795	8	C	-0.181796
9	C	-0.193874	9	C	-0.196839

10	C	-0.193892	10	C	-0.218404
11	C	-0.193971	11	C	-0.057321
12	H	0.147046	12	C	0.408244
13	H	0.147023	13	O	-0.423211
14	H	0.147059	14	C	-0.549185
15	H	0.147037	15	H	0.160343
16	H	0.147022	16	H	0.153592
17	H	0.147042	17	H	0.152225
18	H	0.147019	18	H	0.150032
19	H	0.147049	19	H	0.161054
20	H	0.147041	20	H	0.171781
21	H	0.147009	21	H	0.152821
			22	H	0.152217
			23	H	0.147457
			24	H	0.171524
			25	H	0.172445
			26	H	0.177565

This implies that the effect of  $-\text{COCH}_3$  group on the Cp ring of acetyl ferrocene is negligible. The charge on iron increases slightly in acetyl ferrocene, presumably due to higher electron donation from Fe to SCp ring in presence of a  $-\text{COCH}_3$  group. This is further justified from the HOMO-LUMO analysis which will be discussed in the next section. In case of acetyl ferrocene, the amount of negative charge on  $\text{C}_{11}$  has decreased drastically as compared to that of the rest of the ring carbons, most likely due to the presence of a highly electronegative oxygen atom on the adjacent  $-\text{COCH}_3$  group.

### 3.3. Frontier Molecular Orbital Analysis

The highest occupied molecular orbitals (HOMO) and the lowest unoccupied molecular orbitals (LUMO) are called the frontier molecular orbitals (FMO). The HOMO orbital acts as an electron donor whereas the LUMO orbital acts as an electron acceptor. The HOMO-LUMO energy gap ( $\Delta E_{\text{HOMO-LUMO}}$ ) provides useful information about charge transfer, stability and chemical reactivity of a molecule [10,17,18]. It is observed that smaller the energy gap between the HOMO and the LUMO, greater is the ease with which electron transfer processes can take place [19, 20].

The HOMO and LUMO orbitals of ferrocene and acetyl ferrocene are shown in Figure 3 to Figure 6. In these plots, red color indicates negative charge and green color represents positive charge. In the HOMO orbitals of both the title compounds, the electron density is mainly localized on the transition metal. But LUMO orbital of ferrocene shows a significant amount of charge

built-up on both the cyclopentadienyl rings. Interestingly in case of LUMO of acetyl ferrocene, the charge is predominantly localized on the acetyl group.

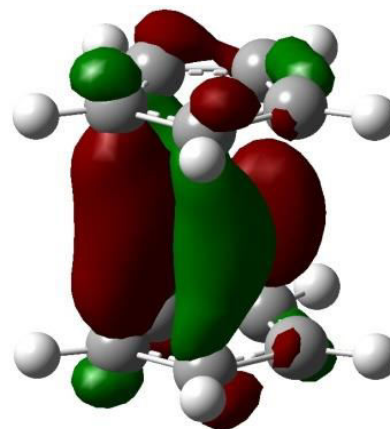


Fig. 3: Ferrocene HOMO

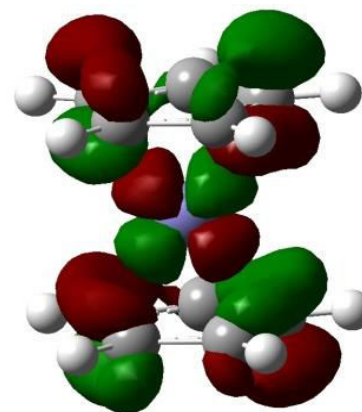
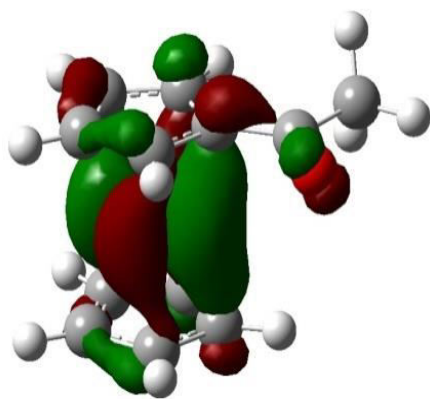
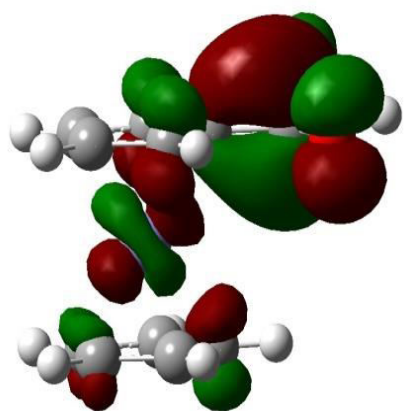


Fig. 4: Ferrocene LUMO



**Fig. 5: Acetyl Ferrocene HOMO**



**Fig. 6: Acetyl ferrocene LUMO**

The HOMO and LUMO energies of eclipsed ferrocene are estimated to be  $-0.19006$  a.u. and  $0.00930$  a.u. respectively. The corresponding HOMO-LUMO energy gap is calculated to be approximately  $5.42$  eV which is in good agreement with the results obtained by Narges et al. [9]. Similarly the HOMO and LUMO energies of the eclipsed conformer of acetyl ferrocene are estimated to be  $-0.20361$  a.u. and  $-0.03380$  a.u. respectively. In this case the, the calculated HOMO-LUMO energy gap is approximately  $4.62$  eV. Hence the HOMO-LUMO energy gap decreases significantly when a hydrogen atom of ferrocene is replaced by an acetyl group.

In order to confirm the effect of substitution [10], the HOMO and LUMO energies of the cyclopentadienyl anion ( $\text{Cp}^-$ ) and the substituted cyclopentadienyl anion ( $\text{SCp}^-$ ) are calculated using B3LYP/6-31G\* method. The energies of the HOMO and LUMO of the cyclopentadienyl anion are computed to be  $0.04132$  a.u. and  $0.30351$  a.u. respectively whereas those of acetyl

substituted cyclopentadienyl anion are found to be  $0.00303$  a.u. and  $0.16984$  a.u. respectively. Thus after substitution LUMO energy of acetyl substituted cyclopentadienyl anion drops considerably. This clearly indicates that after substitution, interaction between the d orbitals of iron and the  $\pi$  orbitals of the ligand will be much better in case of acetyl ferrocene. This is further justified from the NBO analysis.

### 3.4. MEP Analysis

Molecular electrostatic potential (MEP) is a mapping technique which helps to visualize the distribution of electronic charge within the molecules. It is used to identify the active sites which are susceptible to nucleophilic and electrophilic attacks. The MEP plots of the eclipsed conformers of ferrocene and acetyl ferrocene are shown in fig. 7 and 8. In these plots red color refers to electron-rich (negative) region, blue color refers to electron-deficient (positive) region and green color represents zero electrostatic potential.

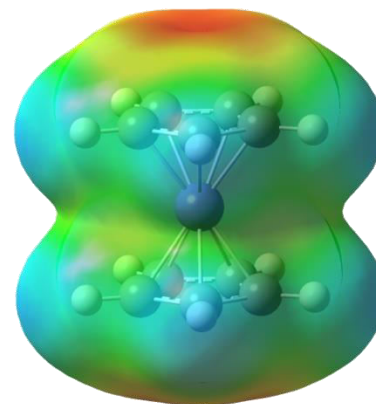


**Fig. 7: MEP mapping of eclipsed ferrocene**

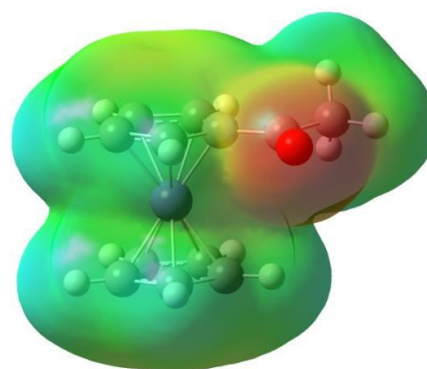


**Fig. 8: MEP mapping of eclipsed acetyl ferrocene**

For an isovalue of 0.001, the negative and positive electron density varies within the range of  $-3.07 \times 10^{-2}$  a.u. to  $3.07 \times 10^{-2}$  a.u. for ferrocene and  $-6.14 \times 10^{-2}$  a.u. to  $6.14 \times 10^{-2}$  a.u. for acetyl ferrocene. From these plots it is obvious that ferrocene is more susceptible to electrophilic attack than acetyl ferrocene where negative charge is predominantly localized on the acetyl group. The electrophile is expected to attack the oxygen atom of the acetyl group.

### 3.5. NBO Analysis

In order to understand the electronic structure and hybridization of the atoms of the title molecules, NBO calculations are performed. It is observed that the interaction energies between the two cyclopentadienyl rings of both compounds are very small. This indicates that there is virtually no direct interaction between the two rings.

#### 3.5.1. Natural Population Analysis

Natural population analysis [21] is performed on the B3LYP/6-31G\* optimized geometries of the eclipsed conformers of ferrocene and acetyl ferrocene. It shows the distribution of electrons in various sub-shells of the

orbitals. The distribution of charges on the individual atoms and the accumulation of electrons in the core, valence and Rydberg sub-shells are shown in table 3.

From table 3 we see that in case of ferrocene, the most electropositive charge of 0.62396e is accumulated on iron but the amount of electronegative charge is almost same on all the carbon atoms of both the cyclopentadienyl rings, which indicates extensive delocalization throughout the rings. In case of acetyl ferrocene, the most electropositive atom is Fe<sub>6</sub> (0.64831e) which is followed by C<sub>12</sub> (0.57527e) that is attached to the electronegative oxygen atom. Interestingly C<sub>14</sub> accumulates more negative charge (-0.75802e) than O<sub>13</sub> (-0.55725e). From the perspective of electrostatic interaction, electronegative atoms have a tendency to donate electrons, whereas electropositive atoms have a tendency to accept electrons. This clearly indicates that when a hydrogen atom of ferrocene is replaced by a -COCH<sub>3</sub> group, both electron donating and electron accepting properties of acetyl ferrocene are enhanced. This is further justified from the NBO analysis. Natural population analysis shows that the electrons of ferrocene and acetyl ferrocene are distributed in various sub-shells as shown in table 4.

**Table 3: Accumulation of natural charges, population of electrons in core, valence and Rydberg orbitals of ferrocene and acetyl ferrocene**

Ferrocene (eclipsed)						Acetyl Ferrocene (eclipsed)					
Atom No.	Natural Charge (e)	Natural population (e)			Total (e)	Atom No.	Natural Charge (e)	Natural population (e)			Total (e)
		Core	Valence	Rydberg				Core	Valence	Rydberg	
C <sub>1</sub>	-0.32138	1.99875	4.30043	0.02219	6.32138	C <sub>1</sub>	-0.31630	1.99875	4.29532	0.02223	6.31630
C <sub>2</sub>	-0.32139	1.99875	4.30045	0.02219	6.32139	C <sub>2</sub>	-0.31704	1.99875	4.29630	0.02199	6.31704
C <sub>3</sub>	-0.32142	1.99875	4.30047	0.02219	6.32142	C <sub>3</sub>	-0.31834	1.99875	4.29748	0.02211	6.31834
C <sub>4</sub>	-0.32135	1.99875	4.30041	0.02219	6.32135	C <sub>4</sub>	-0.32287	1.99875	4.30197	0.02214	6.32287
C <sub>5</sub>	-0.32143	1.99875	4.30049	0.02220	6.32143	C <sub>5</sub>	-0.31305	1.99875	4.29211	0.02219	6.31305
Fe <sub>6</sub>	0.62396	17.99528	7.36514	0.01562	25.37604	Fe <sub>6</sub>	0.64831	17.99461	7.34165	0.01543	25.35169
C <sub>7</sub>	-0.32133	1.99875	4.30039	0.02219	6.32133	C <sub>7</sub>	-0.28043	1.99872	4.25834	0.02337	6.28043
C <sub>8</sub>	-0.32134	1.99875	4.30039	0.02219	6.32134	C <sub>8</sub>	-0.31026	1.99876	4.28959	0.02190	6.31026
C <sub>9</sub>	-0.32140	1.99875	4.30046	0.02219	6.32140	C <sub>9</sub>	-0.31245	1.99876	4.29111	0.02259	6.31245
C <sub>10</sub>	-0.32143	1.99875	4.30048	0.02219	6.32143	C <sub>10</sub>	-0.30350	1.99873	4.28414	0.02063	6.30350
C <sub>11</sub>	-0.32146	1.99875	4.30051	0.02220	6.32146	C <sub>11</sub>	-0.23671	1.99858	4.21348	0.02466	6.23671
H <sub>12</sub>	0.25901	0.00000	0.74014	0.00085	0.74099	C <sub>12</sub>	0.57527	1.99903	3.38735	0.03836	5.42473
H <sub>13</sub>	0.25897	0.00000	0.74018	0.00085	0.74103	O <sub>13</sub>	-0.55725	1.99973	6.54012	0.01740	8.55725
H <sub>14</sub>	0.25901	0.00000	0.74014	0.00085	0.74099	C <sub>14</sub>	-0.75802	1.99923	4.75148	0.00731	6.75802
H <sub>15</sub>	0.25900	0.00000	0.74016	0.00085	0.74100	H <sub>15</sub>	0.26600	0.00000	0.73316	0.00083	0.73400
H <sub>16</sub>	0.25901	0.00000	0.74014	0.00085	0.74099	H <sub>16</sub>	0.26167	0.00000	0.73746	0.00087	0.73833
H <sub>17</sub>	0.25901	0.00000	0.74014	0.00085	0.74099	H <sub>17</sub>	0.26112	0.00000	0.73801	0.00087	0.73888
H <sub>18</sub>	0.25897	0.00000	0.74018	0.00085	0.74103	H <sub>18</sub>	0.26043	0.00000	0.73871	0.00087	0.73957
H <sub>19</sub>	0.25900	0.00000	0.74015	0.00085	0.74100	H <sub>19</sub>	0.26523	0.00000	0.73386	0.00091	0.73477
H <sub>20</sub>	0.25900	0.00000	0.74015	0.00085	0.74100	H <sub>20</sub>	0.27588	0.00000	0.72257	0.00155	0.72412
H <sub>21</sub>	0.25900	0.00000	0.74015	0.00085	0.74100	H <sub>21</sub>	0.26251	0.00000	0.73667	0.00082	0.73749
						H <sub>22</sub>	0.26189	0.00000	0.73726	0.00085	0.73811
						H <sub>23</sub>	0.26163	0.00000	0.73748	0.00089	0.73837
						H <sub>24</sub>	0.24239	0.00000	0.75646	0.00115	0.75761
						H <sub>25</sub>	0.24850	0.00000	0.75049	0.00101	0.75150
						H <sub>26</sub>	0.25541	0.00000	0.74272	0.00187	0.74459

### 3.5.2. Natural bond orbital analysis

The natural bond analysis [22, 23] provides a way to visualize the delocalization of electron density from the occupied Lewis-type (bonding or lone pair) orbitals to unoccupied non-Lewis (anti-bonding or Rydberg) orbitals. For each pair of donor NBO ( $i$ ) and acceptor NBO ( $j$ ), stabilization energy is expressed in terms of second order perturbation interaction energy,  $E(2)$ , by the following relation

$$E(2) = \Delta E_{ij} = q_i \frac{F(i,j)^2}{\epsilon_j - \epsilon_i}$$

where  $q_i$  is the donor orbital occupancy,  $\epsilon_i$  and  $\epsilon_j$  are the diagonal elements and  $F(i,j)$  is the off-diagonal NBO Fock matrix element [24]. Thus NBO analysis provides useful information regarding intra- and intermolecular bonding and interactions among various

bonds within the molecule. Larger the value of  $E(2)$ , stronger is the interaction between the donor and the acceptor.

Results of NBO analysis are summarized in table 5 and table 6. Table 5 shows the occupancies and the percentage of hybrid atomic orbitals of the most interacting NBOs for the eclipsed conformers of both ferrocene and acetyl ferrocene. From table 5 we see that in case of both ferrocene and acetyl ferrocene, bonding and antibonding orbitals of carbon atoms are predominantly contributed by p orbitals whereas those of the iron atom are mainly contributed by d orbitals.

Table 6 summarizes the most interacting NBOs of the eclipsed conformers of ferrocene and acetyl ferrocene along with the corresponding second order perturbation energies, which are also known as stabilization energies or interaction energies.

**Table 4: Percentage of distribution of electrons in core, valence and Rydberg orbitals**

	Ferrocene	Acetyl ferrocene
Core	37.98280 (99.9547% of 38)	43.97990 (99.9543% of 44)
Valence	57.77115 (99.6054% of 58)	73.70529 (99.6017% of 74)
Rydberg	0.24604 (0.2563% of 96)	0.31480 (0.2668% of 118)

**Table 5: Natural atomic orbital occupancies of most interacting NBOs and the percentage of hybrid atomic orbitals of ferrocene and acetyl ferrocene**

		Ferrocene		
NBO	Occupancies	Hybrid	AO (%)	
$\pi(C_1 - C_2)$	1.60557	p	s (2.16%)	p (97.73%) d (0.11%)
$\pi(C_3 - C_4)$	1.60575	p	s (2.16%)	p (97.73%) d (0.11%)
$\pi(C_7 - C_{11})$	1.60554	p	s (2.16%)	p (97.73%) d (0.11%)
$\pi(C_8 - C_9)$	1.60555	p	s (2.16%)	p (97.73%) d (0.11%)
$n_1 C_5$	1.06367	p	s (4.87%)	p (95.05%) d (0.08%)
$n_2 Fe_6$	1.69472	d	s (0.00%)	p (0.00%) d (100.00%)
$n_3 Fe_6$	1.69434	d	s (0.00%)	p (0.00%) d (100.00%)
$n_4^* Fe_6$	0.70218	d	s (0.00%)	p (0.00%) d (100.00%)
$n_5^* Fe_6$	0.70201	d	s (0.00%)	p (0.00%) d (100.00%)
$n_1 C_{10}$	1.06366	p	s (4.86%)	p (95.06%) d (0.08%)
$\pi^*(C_1 - C_2)$	0.53654	p	s (2.16%)	p (97.73%) d (0.11%)
$\pi^*(C_3 - C_4)$	0.53634	p	s (2.16%)	p (97.73%) d (0.11%)
$\pi^*(C_7 - C_{11})$	0.53656	p	s (2.16%)	p (97.73%) d (0.11%)
$\pi^*(C_8 - C_9)$	0.53653	p	s (2.16%)	p (97.73%) d (0.11%)
		Acetyl Ferrocene		
NBO	Occupancies	Hybrid	AO (%)	
$\pi(C_1 - C_5)$	1.59935	p	s (2.04%)	p (97.84%) d (0.12%)
$\pi(C_2 - C_3)$	1.60102	p	s (2.12%)	p (97.76%) d (0.12%)
$\pi(C_7 - C_8)$	1.60532	p	s (2.08%)	p (97.80%) d (0.12%)
$\pi(C_9 - C_{10})$	1.61305	p	s (2.03%)	p (97.85%) d (0.12%)
$n_1 C_4$	1.06308	p	s (4.68%)	p (95.23%) d (0.08%)
$n_3 Fe_6$	1.66645	d	s (0.00%)	p (0.01%) d (99.99%) f (0.00%)
$n_4^* Fe_6$	0.71370	d	s (0.00%)	p (0.00%) d (100.00%) f (0.00%)

$n_1 C_{11}$	1.10222	p	s( 3.81%) p ( 96.15%) d ( 0.04%)
$\pi^*(C_1 - C_5)$	0.52136	p	s( 2.04%) p ( 97.84%) d ( 0.12%)
$\pi^*(C_2 - C_3)$	0.52961	p	s( 2.12%) p ( 97.76%) d ( 0.12%)
$\pi^*(C_7 - C_8)$	0.49420	p	s( 2.08%) p ( 97.80%) d ( 0.12%)
$\pi^*(C_9 - C_{10})$	0.51500	p	s( 2.03%) p ( 97.85%) d ( 0.12%)

**Table 6: Second order perturbation analysis of the interactions between donor and acceptor orbitals of eclipsed conformers of ferrocene and acetyl ferrocene**

Ferrocene (eclipsed)			Acetyl ferrocene (eclipsed)		
Donor NBO (i)	Acceptor non-Lewis NBO (j)	E(2) kcal/mol	Donor NBO (i)	Acceptor non-Lewis NBO (j)	E(2) kcal/mol
Within unit 1			Within unit 1		
$\pi(C_1 - C_2)$	$n_1 C_5$	64.63	$\pi(C_1 - C_5)$	$n_1 C_4$	65.33
	$\pi^*(C_3 - C_4)$	15.47		$\pi^*(C_2 - C_3)$	15.91
$\sigma(C_1 - C_5)$	$n_1 C_5$	8.83	$\pi(C_2 - C_3)$	$n_1 C_4$	65.03
$\pi(C_3 - C_4)$	$n_1 C_5$	64.63		$\pi^*(C_1 - C_5)$	15.46
	$\pi^*(C_1 - C_2)$	15.48	$\sigma(C_3 - C_4)$	$n_1 C_4$	8.63
$\sigma(C_4 - C_5)$	$n_1 C_5$	8.82	$\sigma(C_4 - C_5)$	$n_1 C_4$	8.63
$n_1 C_5$	$\pi^*(C_1 - C_2)$	53.71	$n_1 C_4$	$\pi^*(C_1 - C_5)$	53.26
	$\sigma^*(C_1 - C_5)$	5.26		$\pi^*(C_2 - C_3)$	53.08
	$\pi^*(C_3 - C_4)$	53.74		$\sigma^*(C_3 - C_4)$	5.01
	$\sigma^*(C_4 - C_5)$	5.26		$\sigma^*(C_4 - C_5)$	4.96
Unit 1 to 2			Unit 1 to 2		
$\sigma(C_1 - C_2)$	$n_9^* Fe_6$	13.53	$\sigma(C_1 - C_2)$	$n_7^* Fe_6$	11.46
$\pi(C_1 - C_2)$	$n_4^* Fe_6$	5.75		$n_8^* Fe_6$	8.85
	$n_5^* Fe_6$	31.82		$n_9^* Fe_6$	8.06
	$n_7^* Fe_6$	11.47	$\sigma(C_1 - C_5)$	$n_8^* Fe_6$	16.07
	$n_8^* Fe_6$	23.58	$\pi(C_1 - C_5)$	$n_4^* Fe_6$	20.15
	$n_9^* Fe_6$	12.97	$\pi(C_1 - C_5)$	$n_5^* Fe_6$	20.33
$\sigma(C_1 - C_5)$	$n_8^* Fe_6$	5.99		$n_7^* Fe_6$	13.26
	$n_9^* Fe_6$	14.60		$n_8^* Fe_6$	30.99
$\sigma(C_2 - C_3)$	$n_8^* Fe_6$	7.05	$\sigma(C_2 - C_3)$	$n_7^* Fe_6$	10.58
	$n_9^* Fe_6$	15.83		$n_9^* Fe_6$	10.69
$\sigma(C_3 - C_4)$	$n_8^* Fe_6$	5.23	$\pi(C_2 - C_3)$	$n_5^* Fe_6$	39.52
	$n_9^* Fe_6$	13.53		$n_7^* Fe_6$	40.55
$\pi(C_3 - C_4)$	$n_5^* Fe_6$	35.56		$n_9^* Fe_6$	12.58
	$n_6^* Fe_6$	11.60	$\sigma(C_3 - C_4)$	$n_7^* Fe_6$	7.33
	$n_8^* Fe_6$	22.83		$n_8^* Fe_6$	6.17
	$n_9^* Fe_6$	12.99		$n_9^* Fe_6$	8.57
$\sigma(C_4 - C_5)$	$n_8^* Fe_6$	5.87	$\sigma(C_4 - C_5)$	$n_8^* Fe_6$	16.67
	$n_9^* Fe_6$	14.60	$\sigma(C_5 - H_{19})$	$n_8^* Fe_6$	8.10
$n_1 C_5$	$n_4^* Fe_6$	139.03	$n_1 C_4$	$n_4^* Fe_6$	119.32
unit 2 to 1				$n_5^* Fe_6$	36.99
$n_2 Fe_6$	$n_1 C_5$	56.12		$n_6^* Fe_6$	13.52
	$\pi^*(C_3 - C_4)$	22.80		$n_7^* Fe_6$	6.60
$n_3 Fe_6$	$n_1 C_5$	47.09		$n_8^* Fe_6$	8.36
	$\pi^*(C_1 - C_2)$	23.54	Unit 2 to 1		
$n_4^* Fe_6$	$\pi^*(C_1 - C_2)$	19.08	$n_2 Fe_6$	$n_1 C_4$	21.55
	$\pi^*(C_3 - C_4)$	21.35		$\pi^*(C_2 - C_3)$	23.23
unit 2 to 3			$n_3 Fe_6$	$n_1 C_4$	64.74
$n_2 Fe_6$	$n_1 C_{10}$	101.40		$\pi^*(C_1 - C_5)$	20.69
	$\pi^*(C_7 - C_{11})$	5.60	$n_4^* Fe_6$	$\pi^*(C_1 - C_5)$	10.61
	$\pi^*(C_8 - C_9)$	11.07		$\pi^*(C_2 - C_3)$	20.61
$n_3 Fe_6$	$\pi^*(C_7 - C_{11})$	18.22	$n_5^* Fe_6$	$\pi^*(C_1 - C_5)$	10.40
	$\pi^*(C_8 - C_9)$	12.73	Within unit 2		
$n_4^* Fe_6$	$\pi^*(C_7 - C_{11})$	9.61	$n_8^* Fe_6$	$n_9^* Fe_6$	85.44

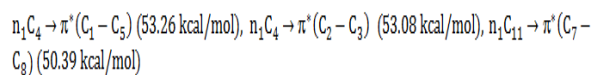
$n_5^* Fe_6$	$\pi^*(C_7 - C_{11})$	12.92	Unit 2 to 3		
	$\pi^*(C_8 - C_9)$	22.36	$n_2 Fe_6$	$\pi^*(C_7 - C_8)$	15.78
unit 3 to 2				$\pi^*(C_9 - C_{10})$	13.09
$\sigma(C_7 - C_8)$	$n_9^* Fe_6$	15.83	$n_3 Fe_6$	$n_1 C_{11}$	88.33
$\sigma(C_7 - C_{11})$	$n_8^* Fe_6$	5.25		$\pi^*(C_7 - C_8)$	8.80
$\sigma(C_7 - C_{11})$	$n_9^* Fe_6$	13.53		$\pi^*(C_9 - C_{10})$	12.11
$\pi(C_7 - C_{11})$	$n_4^* Fe_6$	21.53	$n_5^* Fe_6$	$\pi^*(C_7 - C_8)$	12.47
	$n_5^* Fe_6$	16.02		$\pi^*(C_9 - C_{10})$	17.90
	$n_6^* Fe_6$	14.51	Unit 3 to 2		
	$n_8^* Fe_6$	22.93	$\sigma(C_7 - C_8)$	$n_9^* Fe_6$	11.78
	$n_9^* Fe_6$	12.97	$\pi(C_7 - C_8)$	$n_4^* Fe_6$	29.94
$\sigma(C_8 - C_9)$	$n_8^* Fe_6$	5.39		$n_5^* Fe_6$	8.69
	$n_9^* Fe_6$	13.53		$n_6^* Fe_6$	9.82
$\pi(C_8 - C_9)$	$n_4^* Fe_6$	37.28		$n_7^* Fe_6$	21.98
	$n_6^* Fe_6$	7.39		$n_9^* Fe_6$	13.34
	$n_7^* Fe_6$	7.04	$\sigma(C_7 - C_{11})$	$n_4^* Fe_6$	22.37
	$n_8^* Fe_6$	23.57	$\sigma(C_8 - C_9)$	$n_7^* Fe_6$	7.23
	$n_9^* Fe_6$	12.97		$n_8^* Fe_6$	12.37
$\sigma(C_9 - C_{10})$	$n_8^* Fe_6$	5.99		$n_9^* Fe_6$	8.92
	$n_9^* Fe_6$	14.58	$\sigma(C_9 - C_{10})$	$n_8^* Fe_6$	6.35
$\sigma(C_{10} - C_{11})$	$n_8^* Fe_6$	5.89		$n_9^* Fe_6$	10.89
	$n_9^* Fe_6$	14.58	$\pi(C_9 - C_{10})$	$n_4^* Fe_6$	35.87
$n_1 C_{10}$	$n_4^* Fe_6$	20.98		$n_6^* Fe_6$	15.92
	$n_5^* Fe_6$	119.14		$n_7^* Fe_6$	13.18
	$n_7^* Fe_6$	8.93		$n_8^* Fe_6$	6.93
	$n_8^* Fe_6$	12.98		$n_9^* Fe_6$	11.93
	$n_9^* Fe_6$	6.63	$\sigma(C_{10} - C_{11})$	$n_9^* Fe_6$	21.95
$\pi^*(C_7 - C_{11})$	$n_7^* Fe_6$	5.05	$\sigma(C_{11} - C_{12})$	$n_9^* Fe_6$	7.12
Within unit 3			$n_1 C_{11}$	$n_5^* Fe_6$	140.56
$\pi(C_7 - C_{11})$	$n_1 C_{10}$	64.64		$n_9^* Fe_6$	18.05
	$\pi^*(C_8 - C_9)$	15.48	Within unit 3		
$\pi(C_8 - C_9)$	$n_1 C_{10}$	64.66	$\pi(C_7 - C_8)$	$n_1 C_{11}$	63.81
	$\pi^*(C_7 - C_{11})$	15.48		$\pi^*(C_9 - C_{10})$	15.97
$\sigma(C_9 - C_{10})$	$n_1 C_{10}$	8.82	$\sigma(C_7 - C_{11})$	$n_1 C_{11}$	7.24
$\sigma(C_{10} - C_{11})$	$n_1 C_{10}$	8.83	$\pi(C_9 - C_{10})$	$n_1 C_{11}$	62.77
$n_1 C_{10}$	$\pi^*(C_7 - C_{11})$	53.74		$\pi^*(C_7 - C_8)$	15.01
	$\pi^*(C_8 - C_9)$	53.76	$\sigma(C_{10} - C_{11})$	$n_1 C_{11}$	7.29
	$\sigma^*(C_9 - C_{10})$	5.27	$\pi(C_{12} - O_{13})$	$n_1 C_{11}$	7.82
	$\sigma^*(C_{10} - C_{11})$	5.27	$n_1 C_{11}$	$\pi^*(C_7 - C_8)$	50.39
				$\pi^*(C_9 - C_{10})$	52.83
				$\pi^*(C_{12} - O_{13})$	40.58
			$n_2 O_{13}$	$\sigma^*(C_{11} - C_{12})$	19.27
				$\sigma^*(C_{12} - C_{14})$	20.29

In case of ferrocene, strong conjugative interactions are observed in both the cyclopentadienyl rings. Extended delocalization over the rings is strongly favoured by the following interactions:  $\pi(C_1 - C_2) \rightarrow n_1 C_5$  (64.63 kcal/mol),  $\pi(C_3 - C_4) \rightarrow n_1 C_5$  (64.63 kcal/mol),  $\pi(C_7 - C_{11}) \rightarrow n_1 C_{10}$  (64.64 kcal/mol), and  $\pi(C_8 - C_9) \rightarrow n_1 C_{10}$  (64.66 kcal/mol). Several hyper conjugative interactions are also observed which impart stability to the rings. A few of such interactions are:  $n_1 C_5 \rightarrow \pi^*(C_1 - C_2)$  (53.71 kcal/mol),  $n_1 C_5 \rightarrow \pi^*(C_3 - C_4)$  (53.74 kcal/mol),  $n_1 C_{10} \rightarrow \pi^*(C_7 - C_{11})$  (53.74 kcal/mol),

and  $n_1 C_{10} \rightarrow \pi^*(C_8 - C_9)$  (53.76 kcal/mol). Apart from these aforesaid interactions, some significant interactions between the transition metal and the cyclopentadienyl rings are also observed which are as follows:

$n_1 C_5 \rightarrow n_4^* Fe_6$  (139.03 kcal/mol),  $n_2 Fe_6 \rightarrow n_1 C_5$  (56.12 kcal/mol),  $n_3 Fe_6 \rightarrow n_1 C_5$  (47.09 kcal/mol) and  $n_2 Fe_6 \rightarrow n_1 C_{10}$  (101.40 kcal/mol). These interactions predominantly involve the d orbital of iron and the p orbital centred on a carbon atom of the ring.

Similar kind of interactions is also observed in acetyl ferrocene. For example, strong conjugative interactions are evidenced by  $\pi(\text{C}_1 - \text{C}_5) \rightarrow n_1\text{C}_4$  (65.33 kcal/mol),  $\pi(\text{C}_2 - \text{C}_3) \rightarrow n_1\text{C}_4$  (65.03 kcal/mol),  $\pi(\text{C}_7 - \text{C}_8) \rightarrow n_1\text{C}_{11}$  (63.81 kcal/mol) and  $\pi(\text{C}_9 - \text{C}_{10}) \rightarrow n_1\text{C}_{11}$  (62.77 kcal/mol). Similarly several hyper conjugative interactions are also observed. A few of such interactions are:



and  $n_1\text{C}_{11} \rightarrow \pi^*(\text{C}_9 - \text{C}_{10})$  (52.83 kcal/mol). Some significant interactions between the metal d orbitals and the p orbitals of carbon of acetyl ferrocene are as follows:  $n_1\text{C}_4 \rightarrow n_4^*\text{Fe}_6$  (119.32 kcal/mol),  $n_3\text{Fe}_6 \rightarrow n_1\text{C}_4$  (64.74 kcal/mol),  $n_3\text{Fe}_6 \rightarrow n_1\text{C}_{11}$  (88.33 kcal/mol) and  $n_1\text{C}_{11} \rightarrow n_5^*\text{Fe}_6$  (140.56 kcal/mol). Thus NBO analysis clearly indicates that the donor-acceptor interactions involve charge transfer from metal to ligand and back-donation from ligand to metal. The observed increase in interaction energies in acetyl ferrocene, although by a small amount, suggests stronger donor-acceptor interactions than in ferrocene. This is further supported from Mulliken charge analysis and Natural Population Analysis.

### 3.6. Theoretical study of UV-VIS spectra

In order to study the electronic transitions between various energy levels and theoretically simulate the UV-

VIS spectra, TDDFT calculations are performed on the B3LYP/6-31G\* optimized geometries of the eclipsed conformers of both ferrocene and acetyl ferrocene. Ten lowest excitation states of each compound are computed. The simulated spectra of both compounds are shown in fig.9 and fig. 10. In case of ferrocene a single intense peak is observed at 221.92 nm with oscillator strength ( $f$ ) of 0.0099 a.u. This band mainly originates from several transitions like HOMO-1 to LUMO+7, HOMO-1 to LUMO+8 and HOMO to LUMO+7. Based on previous TDDFT studies [23-25], this band may be assigned to  $\pi \rightarrow \pi^*$  transition.

In case of acetyl ferrocene, two absorption bands are observed. The first intense band mainly results from HOMO-3 to LUMO, HOMO-1 to LUMO+2 and HOMO to LUMO+2 transitions. The oscillator strengths of these transitions are significantly large. The less intense broad second band mainly results from several transitions like HOMO-1 to LUMO, HOMO to LUMO and HOMO-1 to LUMO+1. The oscillator strengths of these transitions are relatively small. Based on previous TDDFT studies [25-27], the first band may be assigned to  $\pi \rightarrow \pi^*$  transition and the second band may be assigned to Metal to Ligand Charge Transfer (MLCT) transition.

**Table 7: Selected simulated optical transitions of eclipsed conformers of ferrocene and acetyl ferrocene**

Molecule	Excitation	$\lambda_{\text{max}}$ (nm)	$\Delta E$ (eV)	$f$ (a.u.)
Ferrocene	HOMO - 1 $\rightarrow$ LUMO + 7	221.92	5.5869	0.0099
	HOMO - 1 $\rightarrow$ LUMO + 8	221.91	5.5873	0.0100
	HOMO $\rightarrow$ LUMO + 7	221.91	5.5873	0.0100
Acetyl Ferrocene	HOMO - 3 $\rightarrow$ LUMO	311.41	3.9814	0.0012
	HOMO - 1 $\rightarrow$ LUMO + 2	308.36	4.0208	0.0014
	HOMO $\rightarrow$ LUMO + 2	291.29	4.2564	0.0226
	HOMO - 1 $\rightarrow$ LUMO	534.85	2.3181	0.0001
	HOMO $\rightarrow$ LUMO	528.58	2.3456	0.0013
	HOMO - 1 $\rightarrow$ LUMO + 1	476.37	2.6027	0.0003

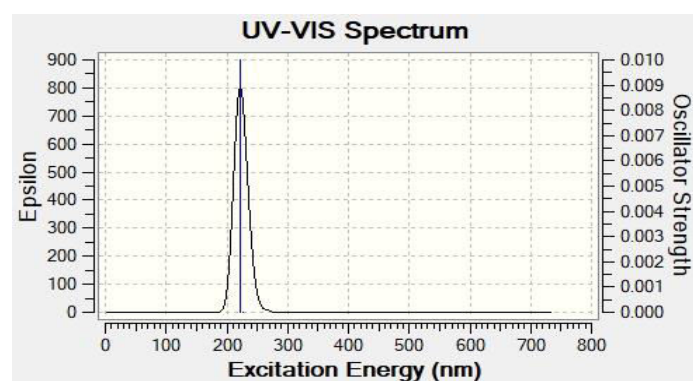


**Fig. 9: UV VIS spectrum of eclipsed ferrocene**

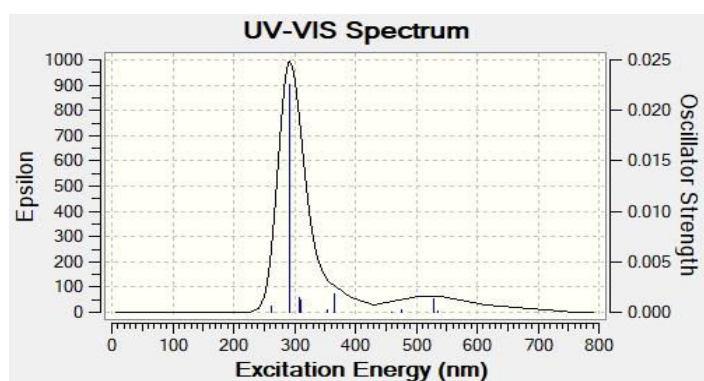


**Fig. 10: UV VIS spectrum of eclipsed acetyl ferrocene**

#### 4. CONCLUSION

Ferrocene and acetyl ferrocene are studied in the gas phase using density functional B3LYP model with 6-31G\* basis set. For both the title compounds, the eclipsed conformer is found to be the most stable structure. The difference in energy between the eclipsed and staggered conformers of ferrocene and acetyl ferrocene are calculated to be approximately 0.58 kJ/mol and 0.82 kJ/mol respectively. Mulliken charge analysis shows that the iron atom of the title compounds carry a positive charge. But in case of acetyl ferrocene, this charge has increased significantly, presumably due to higher electron donation from Fe to SCp ring in presence of -COCH<sub>3</sub> group.

The HOMO-LUMO energy gaps of the eclipsed conformers of ferrocene and acetyl ferrocene are calculated to be 5.42 and 4.62 eV respectively. In case of HOMO orbitals of both the title compounds, the electron density is mainly localized on the transition metal. But LUMO orbital of ferrocene shows a significant amount of charge built-up on both the cyclopentadienyl rings. But in case of LUMO of acetyl ferrocene, the charge is predominantly localized on the acetyl group.

NBO analysis shows that for both the title compounds, direct interaction between the two cyclopentadienyl rings is negligible. Natural population analysis shows that extensive delocalization occurs throughout both the cyclopentadienyl rings of each compound. The second order perturbation result of NBO analysis identifies the most significant hyper conjugative and conjugative interactions that provide stability to the molecules. Some significant interactions between the transition metal and the cyclopentadienyl rings are also observed in both the compounds.

The simulated UV-VIS spectra show that ferrocene has a single intense peak which is assigned to  $\pi \rightarrow \pi^*$  transition. Acetyl ferrocene has one large intense peak along with a broad less intense shoulder. These bands are assigned to  $\pi \rightarrow \pi^*$  and MLCT transitions respectively. All the electronic transitions and the corresponding MOs, which account for these peaks, are identified. Thus the present study provides a better understanding of the geometrical and electronic properties of ferrocene and acetyl ferrocene to a greater extent.

#### 5. ACKNOWLEDGEMENTS

The author would like to thank Dr. Prabhuram Khatua (Retd.) and Prof. Subhabrata Mabhai of Mahishadal Raj

College and Dr. Siddhartha Samanta of K. K. College of Engineering and Management, Dhanbad for their help and support.

#### Conflict of interest

The author declares that there is no conflict of interest.

#### 6. REFERENCES

1. Yamaguchi Y, Palmer BJ, Kutal C, Wakamatsu T, Yang DB. *Macromolecules*, 1998; **31**:5155-5157.
2. Fischer EO, Pfab W. *Z Naturforsch*, 1952; **B7**:377-379.
3. Eiland PF, Pepinsky R. *J Am Chem Soc*, 1952; **74**:4971.
4. Dunitz JD, Orgel LE. *Nature*, 1953; **171**:121-122.
5. Dunitz JD, Orgel LE, Rich A. *Acta Cryst*, 1956; **9**:373-375.
6. Bohn RK, Haaland A. *J Organomet Chem*, 1966; **5**:470-476.
7. Haaland A, Nilsson JE. *Acta Chem Scand*, 1968; **22**: 2653-2670.
8. Haaland A, Luszyk J, Novak DP, Brunvoll J, Starowieyski KB. *J Chem Soc Chem Commun*, 1974; 54-55.
9. Narges M, Aravindhan G, Christopher TC, Feng W. *J Organomet Chem*, 2012; **713**:51-59.
10. Guiling Z, Hui Z, Miao S, Yanhong L, Xiaohong P, Xiaohong P et al. *J Comput Chem*, 2007; **28**: 2260 - 2274.
11. Shawkat I, Feng W. *Royal Soc Chem Adv*, 2015; **5**:11933-11941.
12. Frisch MJ, Trucks GW, Schlegel HB, Scuseria GE, Robb MA, Cheeseman JR et al. Gaussian 09, Revision A.1, Gaussian, Inc., Wallingford CT, 2009.
13. Frish A, Nielsen AB, Holder AJ. Gauss View User Manual, Gaussian Inc., Pittsburg, PA, 2001.
14. Bohn RK, Haaland A. *J Organomet Chem*, 1966; **5**:470-476.
15. Sidis I, Sidir YG, Kumalar M, Tasal E. *J Mol Struct*, 2010; **964**:134-151.
16. Chinniagounder T, Rangaswamy M. *Int J Chem Sci*, 2016; **14**(4):2029-2050.
17. Asiri AM, Karabacak M, Kurt M, Alamry KA. *Spectro Chim Acta A*, 2011; **82**(1):444-455.
18. Liu JN, Chen ZR, Yuan SF. *J Zhejiang. Univ Sci B*, 2005; **6**(6):584-589.
19. K. Fukui. Theory of Orientation and Stereo-selection, Reactivity and Structure, Concepts in

- Organic Chemistry. Berlin: Springer Publishers; 1975.
20. Abou-Rachid H, Song Y, Hu A, Dudiy S, Zybin SV, Goddard WA. *J Phys Chem A*, 2008; **112(46)**:11914-11920.
  21. Reed AE, Weinstock RB, Weinhold F. *J Chem Phys*, 1985; **83**:735.
  22. Keresztury G, Holly S, Varga J, Besenyi G, Wang AV, Durig JR. *Spectrochim Acta*, 1993; **49A**:2007.
  23. Foster JP, Weinhold F. *J Am Chem Soc*, 1980; **102**:7211-7218.
  24. Szafran M, Komasa A, Adamska EB. *J Mol Struct (Theochem)*, 2007; **827**:101-107.
  25. Yong LL, Lei H, Ye M, John ZHZ. *Chem Phys Lett*, 2009; **482**:217-222.
  26. Wen-Wei Z, Yong-Guang Y, Zhen-Da L, Wei-Li M, Yi-Zhi L, Qing-Jin M. *Organometallic*, 2007; **26**:865-873.
  27. Ye-Dong P, Lin-Sen Z, Li-Li C, Lu M, Yue Z, Wen-Wei Z et al. *Dalton Trans*, 2015; **44**:14465-14474.